

Article

Experimental and Simulation Analysis of Warm Shearing Process Parameters for Rolled AZ31B Magnesium Alloy Plate

Yue Meng ^{1,2} , Lifeng Ma ^{1,2,*} and Weitao Jia ^{1,2,*}

¹ College of Mechanical Engineering, Taiyuan University of Science and Technology, Taiyuan 030024, China; my1993@stu.tyust.edu.cn

² Heavy Machinery Engineering Research Center, Ministry of Education, Taiyuan University of Science and Technology, Taiyuan 030024, China

* Correspondence: malifengfqh@163.com (L.M.); jwt860520@163.com (W.J.)

Abstract: The study was carried out on a KRUMAN-CLS1016-NC shearing machine at a shear temperature of 20 °C to 250 °C and a shear edge clearance of 8% to 10% for a rolled AZ31B magnesium alloy plate with a thickness of 8.35 mm. The height and area share of the bright zone in the shear section were analyzed by macroscopic measurements and super depth-of-field experiments, and combined with DEFORM-3D finite element simulations, the optimal shear program was determined using the orthogonal experimental method. It was found that, with the increase of shear temperature and shear edge clearance, the height and area of the burnish band first increased and then decreased. In addition, from the simulated orthogonal test, it can be obtained that the effect of shear temperature on the height of the burnish band is superior to that of the shear edge gap, so the selection of shear temperature is preferred. In this paper, the shear temperature of 150 °C and the shear edge clearance of 12% were finally determined as the best shear process parameters for the rolled AZ31B magnesium alloy sheet.

Keywords: AZ31B magnesium; thermal shearing; shear temperature; shear edge clearance; finite element simulation; orthogonal test



Citation: Meng, Y.; Ma, L.; Jia, W. Experimental and Simulation Analysis of Warm Shearing Process Parameters for Rolled AZ31B Magnesium Alloy Plate. *Crystals* **2022**, *12*, 661. <https://doi.org/10.3390/cryst12050661>

Academic Editor: Pavel Lukáč

Received: 1 April 2022

Accepted: 28 April 2022

Published: 5 May 2022

Publisher's Note: MDPI stays neutral with regard to jurisdictional claims in published maps and institutional affiliations.



Copyright: © 2022 by the authors. Licensee MDPI, Basel, Switzerland. This article is an open access article distributed under the terms and conditions of the Creative Commons Attribution (CC BY) license (<https://creativecommons.org/licenses/by/4.0/>).

1. Introduction

Magnesium is one of the most abundant elements on Earth, with significant levels in the surface of the Earth's crust and in salt lakes and oceans. As they say, "In the field of materials, there is no material that has such an inversion of potential and reality as magnesium [1]." Therefore, in today's scarce metal resources, accelerating the development of magnesium materials is one of the important measures to achieve sustainable development. In the Second World War, thousands of tons of magnesium alloy sheets were used in large quantities in aircraft fuselages, wings, and structural frame members. The use in the automotive industry also increased fourfold over the next 80 years or so, for example in applications such as body panels and internal engine components. However, until now, magnesium alloy sheets have not realized, or fulfilled, the potential of their industrial, civil, or military applications [2], as well as the development of new potentials still to be explored.

At present, the magnesium alloy plate in the production process of the sizing process is all sawing. However, the loss of sawing is more serious, as the resulting debris is flammable and explosive, so there is a great safety hazard. However, if the shearing process can be used in the precision sizing and undercutting of magnesium alloy plates will solve the problems caused by sawing, the process will greatly improve the production efficiency, improve the yield of magnesium alloy plate production, and reduce the risk of accidents.

Due to the advantages of high efficiency, low loss, and the low cost of magnesium alloy plate shearing, in the production of subsequent processes, more precision shearing is used for undercutting. Current precision shearing methods can be divided into heating shearing,

high-speed shearing, axial pressure shearing, radial clamping shearing, plastic fatigue shearing, and progressive shearing [3]. Magnesium is a hexagonal close-packed lattice with low structural symmetry, which is characterized by poor plastic deformation ability at room temperature [4], so the magnesium alloy plate needs to be heated for shearing, by controlling the temperature of the magnesium plate to obtain a better section quality of the plate. During the heating and shearing process, the deformation process of the metal near the contour line of the mold can be divided into three stages: the elastic deformation stage, the plastic deformation stage, and the shearing stage [5]. The plate is not plastically deformed except for the metal near the contour line of the mold. After shearing, the plate section can be divided into four parts: rollover band, burnish band, fracture band, and burr band, as shown in Figure 1. The quality of the section is judged by the height and area of the burnish band; the larger the numerical value, the better the quality of the section.

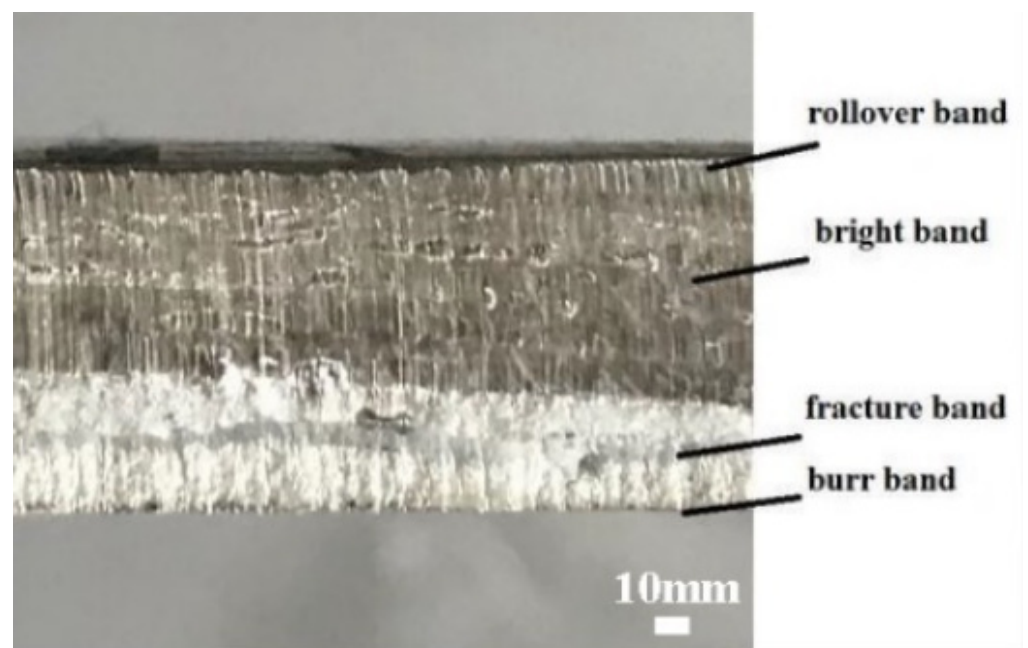


Figure 1. Shearing section of the AZ31B magnesium alloy plate.

In this paper, the shear test was carried out on the same shear machine for the same thickness of magnesium alloy plate, and the section morphology was analyzed at different temperatures as well as the shear edge gap, and verified by simulation, and the orthogonal test analysis method was used to obtain the optimal shearing process parameters for AZ31B magnesium alloy plate after rolling.

2. Materials and Methods

2.1. Experiment Materials

The AZ31B magnesium alloy ingot used in this paper is provided by Shanxi Yinguang Magnesium Industry Group Co. (Yuncheng, China). Its chemical composition is shown in Table 1.

Table 1. AZ31B magnesium alloy sheet element content (wt, %).

Al	Zn	Mn	Fe	Si	Cu	Ni	Mg
3.37	0.86	0.29	0.004	0.1	0.0015	0.0047	Bal.

A specimen of size 100 mm × 150 mm × 12.5 mm was cut from the ingot, and solid solution was treated (400 °C × 12 h); after that, the rolling experiment was carried out on φ350 mill with a rolling temperature of 350 °C–400 °C, rolling speed of 0.25 m/s, and

total depression of 35% (25% depression in the first pass and 10% in the second pass). The final shearing test magnesium plate with a plate thickness of 8.35 mm (mill bounce of ± 0.0885 mm) was obtained, where the roll diameter was 350 mm.

2.2. Thermal Shearing Test

The shearing machine used for the thermal shear experiment was provided by the Jiangsu Jianghai Group with the model number KRUMAN-CLS1016-NC (as shown in Figure 2). In order to ensure the constant temperature of the magnesium plate, this paper adopted the heating method of the LWK-120 KW digital display temperature control box (as shown in Figure 3) connected with heating tape, and after remaining warm for three minutes, temperature detection was carried out by a temperature measuring gun (as shown in Figure 4) with the model number AR842A+ produced by a SMART SENSOR. The magnesium plate specimens obtained in 2.1 were subjected to warm shearing experiments on the shears. Shearing temperature were 20 °C, 100 °C, 150 °C, 200 °C, and 250 °C; shearing edge gap was adjusted initially by 8%, 10%, and 12% of the plate thickness (0.668, 0.835, 1.002), due to the accuracy of the shears adjustment gap is 0.01 (as shown in Figure 5), so 0.7 mm, 0.8 mm, and 1 mm were selected as 8%, 10%, and 12% corresponding to the shearing edge gap; the detailed warm shear experimental program is shown in Table 2.

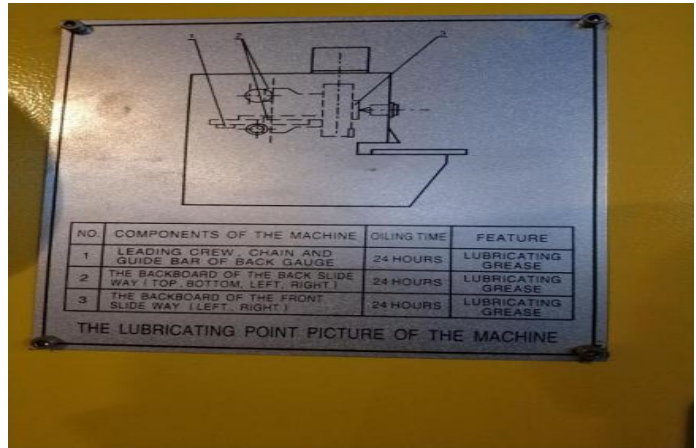


Figure 2. Thermal shearing experimental device.

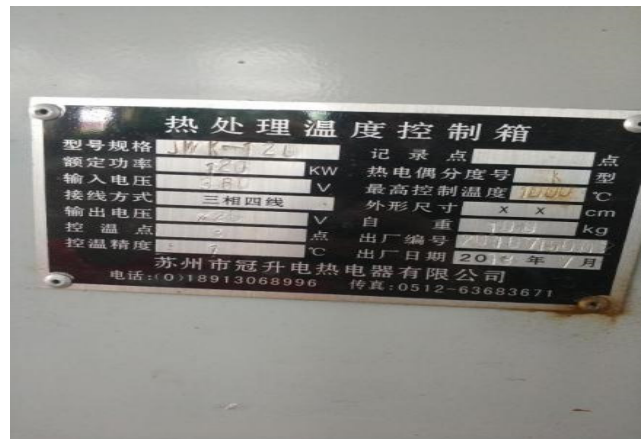


Figure 3. LWK-120 KW digital display temperature control box.



Figure 4. AR842A + temperature gun.



Figure 5. Shear blade clearance setting dial.

Table 2. Thermal shear test scheme.

T	BC	T	BC	T	BC	T	BC	T	BC
20	0.7	100	0.7	150	0.7	200	0.7	250	0.7
20	0.8	100	0.8	150	0.8	200	0.8	250	0.8
20	1	100	1	150	1	200	1	250	1

T—Temperature, Unit—°C; BC—Blade Clearance, Unit—mm.

3. Results

After the shearing test is completed, we conducted preliminary macroscopic analysis of the magnesium plate section and observed its unevenness by a VHX-600E super depth of field microscope, analyzed the effect of different shearing process conditions on the quality of magnesium plate shearing section, and carried out simulation verification by finite element simulation software DEFORM to start orthogonal test analysis.

3.1. Macroscopic Analysis

The macroscopic results of shear fracture specimens under different shearing processes are shown in Table 3, the height of the burnish band of the fracture is shown in Figure 6a, and the area of the burnish band as a percentage is shown in Figure 6b. In the experiments, we measured the maximum height of the bright band on the plate section and calculated the area ratio of the bright band on the whole section to supplement the results. From the figure, it can be found that the shear fracture morphology with different shearing temperature and shearing edge gap has obvious distinction.

Table 3. Macroscopic shear fracture specimens under different shear processes.

BC \ T	T				
	20	100	150	200	250
8%					
10%					
12%					

T—Temperature, Unit—°C; BC—Blade Clearance, Unit—mm.

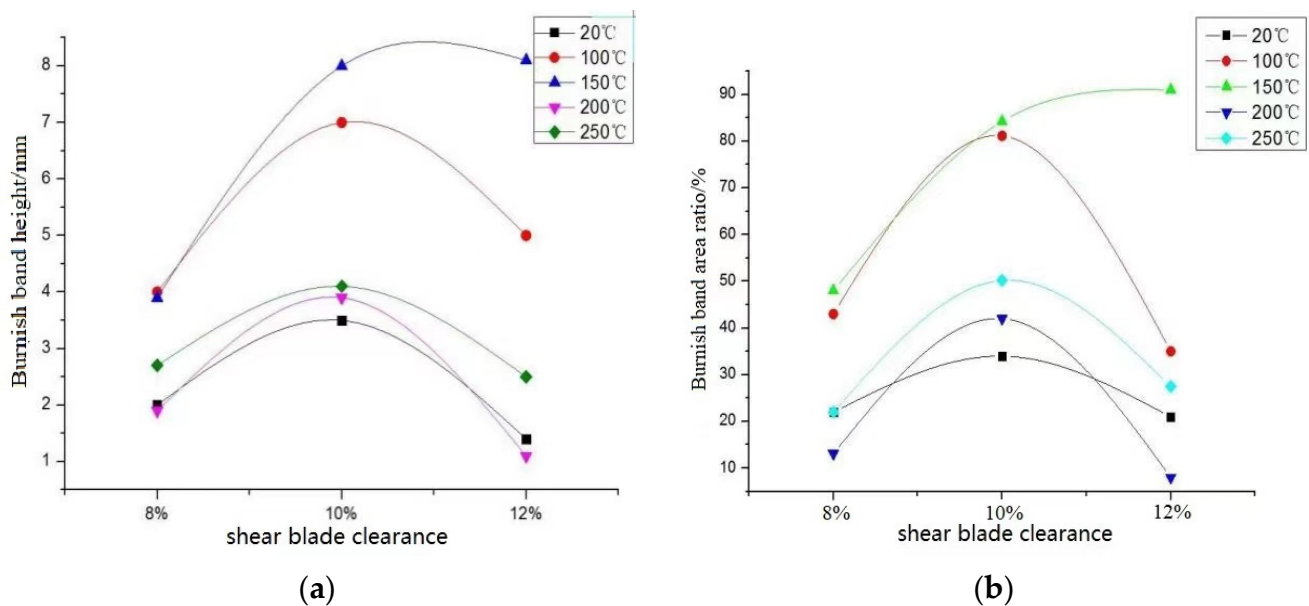


Figure 6. The data analysis of burnish band (a) burnish band height; (b) burnish band area ratio.

3.1.1. Effect of Shearing Temperature

From the macroscopic fracture analysis, it can be seen that the shearing temperature has a significant effect on the shearing section of the magnesium plate.

Under the same shearing edge clearance, when the shearing magnesium plate is at room temperature (20 °C), the plate section has a large number of burrs, the fracture band is larger, the height and area of the burnish band accounted for is smaller, and it can be analyzed that the magnesium alloy of hcp structure in room temperature conditions has a less slip system, which leads to less plasticity, hence the plate section quality is not ideal. At 100 °C, the magnesium plate section has obvious improvement compared with room temperature, burr is reduced, fracture band is decreased, burnish band is increased, and the

height and area ratio of the burnish band is increased significantly. At 150 °C, the fracture band is reduced, the texture is clear and flat, and the height and area of the burnish band of the magnesium plate section reaches the maximum when the same shearing edge gap condition is 10%. At 200 °C, the fracture band increases and the burnish band decreases, and the quality of the section at room temperature is close to that of the section, while the height and area ratio of the burnish band of the section are greatly reduced. At 250 °C, the burnish band height and area percentage of the magnesium plate section slightly reverted to 200 °C, but the burnish band height and area percentage were much less than the shear section at 150 °C.

From the analysis of the results, it can be seen that, with the increase of the shear temperature, the quality of the plate fracture is gradually improved, and when the cutting temperature rises to 150 °C, the quality of the shear section is the best. However, when the temperature continues to rise beyond 150 °C, the section quality gradually decreases. Shearing process is a kind of metal deformation, and dislocation and slippage are the main mechanisms of the shear deformation of the magnesium alloy sheet [6]. Increasing the shear temperature can accelerate the accumulation rate of dislocation density, while increasing the cross-slip shift of dislocations and migration of grain boundaries, increasing the nucleation and growth rate of dynamic re-crystallization, making the critical resolved shear stress decrease, generating dislocation movement, and tangling more easily than at room temperature [7]. At a shear deformation temperature of 150 °C, the main deformation mechanisms of magnesium alloys are low temperature dynamic recrystallization (LTDRX) and twinned dynamic recrystallization (TDRX) [8]. The large strain at this temperature drives the creation of new grain clusters, and these grain boundaries are in an unbalanced state, with so much internal elastic distortion that a large internal stress field is formed. As dislocations continue to accumulate and internal stresses change to critical tangential stresses, non-basal slip will be initiated and large angle recrystallization nuclei will be formed due to rearrangement of dislocations, resulting in a significant refinement of the alloy grain and therefore improved section quality. However, if the temperature continues to rise, to 200–250 °C, magnesium plate section quality will not continue to improve; instead, there will be a significant decline, even when there is shear edge clearance of 8% and 12%, the temperature of the section quality inferior to room temperature conditions. This phenomenon is due to the improvement of plasticity of AZ31 magnesium alloy at 200–250 °C, and, besides the slip on the basal planes in {0001} and <1120>, the angle cone surface {1011} and <1012> also starts to produce slip, so the metal tissue flow is enhanced [9]. At the same time, the main deformation mechanism at medium temperature is continuous dynamic recrystallization (CDRX) [10], that is, due to the accumulation of dislocations at the grain boundaries, the grain boundaries gradually bow out, resulting in the increase of dislocation density at the grain boundaries, the emergence of uneven grain boundary deformation, and the formation of a “necklace-like” organization [11], that is, the phenomenon of medium temperature rheological instability. The phenomenon leads to the formation of small granular protruding surface on the fracture zone, so at 200–250 °C, the quality of the section becomes poor.

3.1.2. Effect of Shear Edge Clearance

The shear edge gap also has a significant effect on the shear section of magnesium plate. In Figure 6, the same shear temperature shear edge clearance can be seen first from 8% to 10%, and the height of the burnish band and area ratio of the change trend are similar. Both tend to increase, with shear edge clearance from 10% to 12%, and the height of the burnish band and area ratio of the relative decreasing. In shear deformation, changing the shear edge clearance will directly lead to changes in the stress distribution in the deformation zone, the generation and expansion of cracks in shear is affected, and the quality of the section is changed. When the shear gap is small, the upper and lower cracks of the plate will be easily staggered outward, and the plate will be easily fractured in advance due to poor grain fluidity, forming step-like bumps, forming burrs and overlaps on the section,

and aggravating the impact on the mold and affecting the mold life [12]. When the shear clearance is too large, the shear edge is not enough to restrain the plate so that bending and upturning occurs, the plastic deformation phase is reduced, and the compressive stress in the metal flow process is transformed into tensile stress, resulting in an increase in the fracture zone and a decrease in the bright zone [13]. Therefore, from the analysis of the results, it is clear that the shear edge clearance should not be too large or too small. Through macroscopic fracture analysis, at the same temperature with 10% shear edge clearance, the section burnish band is larger, and the burr is smaller and flatter, but when the shear temperature is 150 °C, the section quality of 12% shear edge clearance is better than 10% shear edge clearance.

Since twin dynamic recrystallization (TDRX) at 150 °C is one of the main mechanisms of magnesium alloy deformation, twin deformation plays an important coordinating role. At 150 °C, twinning in hcp-structured metals is very sensitive to changes in stress [14]. With the concentration of stress at the grain boundary reaching the critical resolved shear stress (CRSS) required for twinning, twinning is easily generated in large grains, a large number of twins complete nucleation and growth in a short period of time, holes within the grain gradually converge, cracks sprout at the grain boundary of the twin, and the direction of crack extension changes from along a specific crystallographic plane to along the vertical direction of extension [15]. Therefore, when there is shear deformation at this temperature, the appropriate increase in shear edge clearance can stagger outward, the burnish band increases, and the section quality is optimized.

3.2. Experimental Analysis of Super Depth of Field

Ten percent shear clearance, different shear temperatures and 12% shear clearance, and 150 °C shear temperature plate fractures were selected for the analysis of the super depth of field 3D map stitching technique. The experiment was conducted by selecting the same position on the plate for observation, and the magnification was chosen to be 100 times. The results are shown in Table 4. From the comparison results in the table, it can be seen that the area occupied by the lower part of the surface roughness of the fracture at 150 °C under the same cutting edge clearance is the largest and the flatness is the best. In addition, at 150 °C, the surface of the fracture with 12% shear edge clearance is smoother and smoother.

3.3. Orthogonal Test Analysis

The experimental results show that, unlike conventional plate shearing, the shear temperature has a great influence on the shear section quality during the shearing of magnesium alloy plates. In this paper, the two main factors, shear edge clearance and shear temperature, were selected to investigate the effect of shear edge clearance and shear temperature on the cross-sectional quality of the plates in an orthogonal test. Combined with the theoretical analysis, three levels were selected within the study for each of these two factors. From the macroscopic results, it is known that the section quality is better when the shear temperature is from 100 °C to 200 °C, so the parameters of this range are selected, and the detailed parameters are shown in Table 5. According to the number of factors and levels of orthogonal tests in Table 5, an L_9 (3^2) orthogonal table was selected to design a 2-factor, 3-level test.

3.3.1. Simulation Condition

DEFORM-3D finite element software, which is specially designed for metal plastic forming deformation, was used for shear simulation in this paper. As the deformation area during shearing is mainly concentrated in the local shear blade gap, which will lead to distortion of the finite element mesh, the local mesh refinement technique is adopted to divide it, that is, the finite element mesh in the shear blade gap area is densely divided, and in other areas the mesh is relatively sparse. Figure 7 presents a three-dimensional model.

Table 4. Super depth-of-field 3D map.

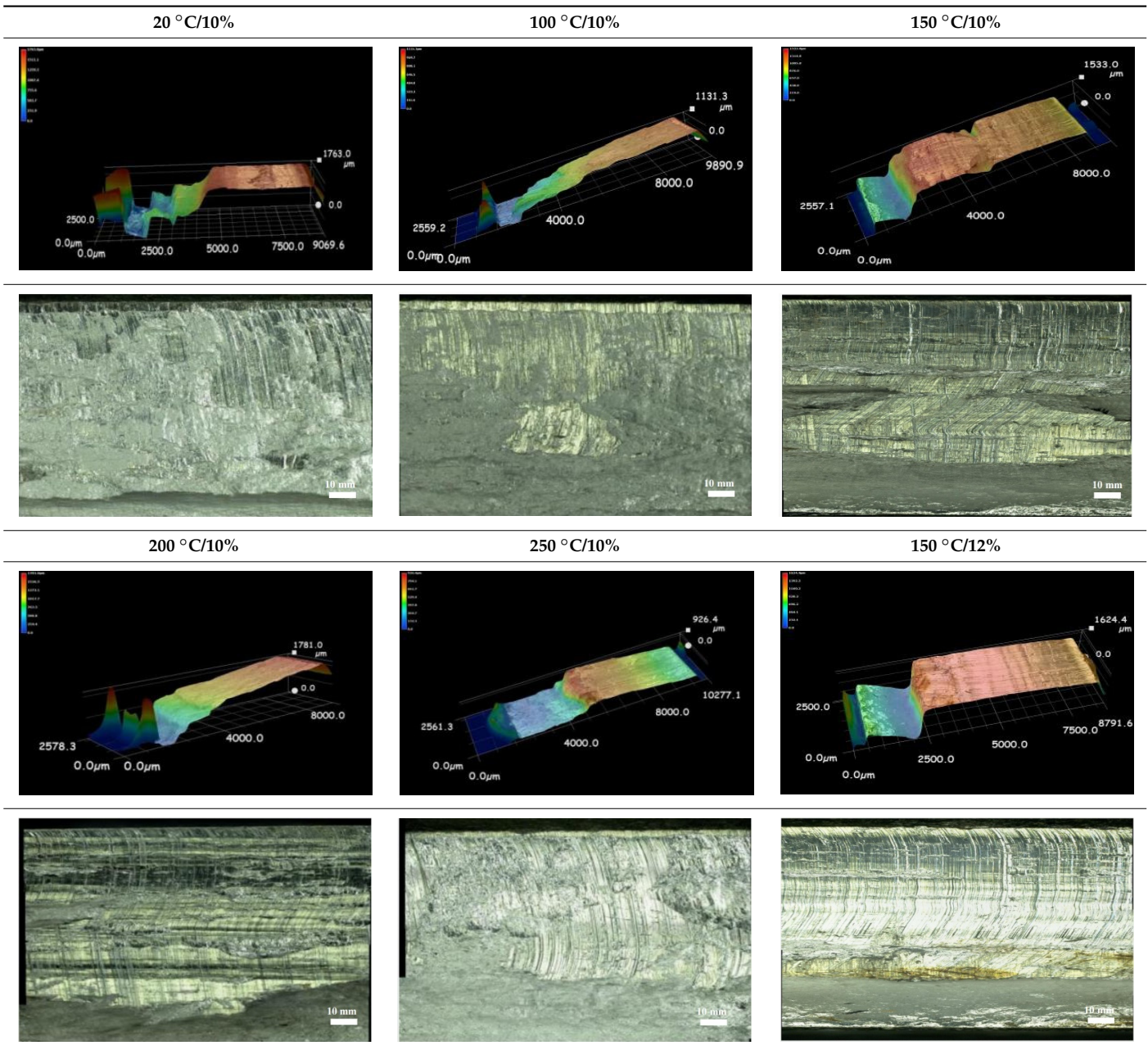


Table 5. Correlation factors and levels of the orthogonal test.

Level	Factor	Blade Clearance (%)	Thermal (°C)
	1	8	100
	2	10	150
	3	12	200

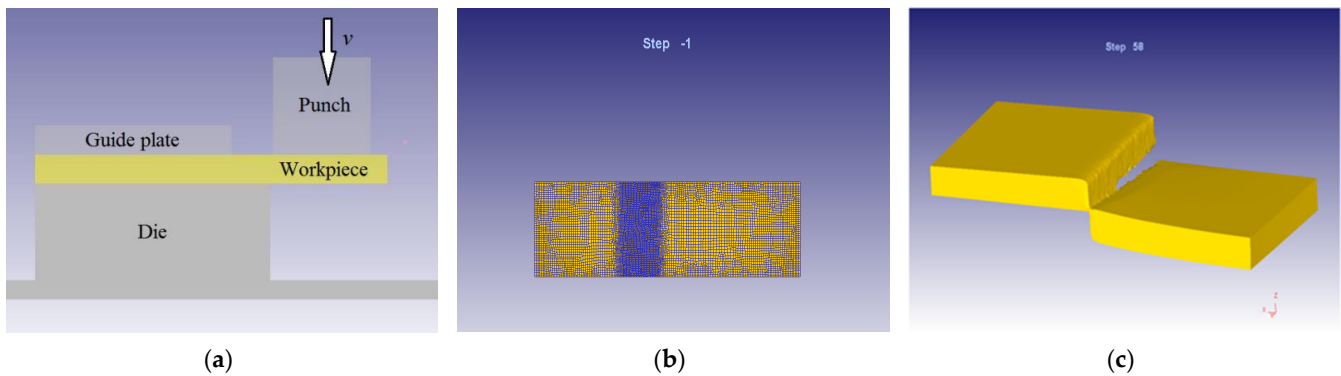


Figure 7. Three-dimensional shear model: (a) modeling; (b) meshing; (c) operating.

The workpiece was set up as a plastic body; at the same time, the punch and die were assumed to be rigid bodies. The cell length of the shear blade clearance area is 0.01 mm, and the other areas are meshed with a larger dimension to improve the computational efficiency. The total number of elements and nodes are 10,057 and 10,300, respectively.

The clearance between the punch and the die was expressed as the ratio of clearance to thickness, c/t_0 ; therefore, shear blade clearance of 0.7, 0.8, and 1.0 mm were selected for the simulation. The blank holding force F_{hold} was 0%, 20%, and 60% of the load added to the punch. The frictional was set to be 0.2.

3.3.2. Material Model and Fracture Criterion Model

The material was assumed to be homogeneous and isotropic in the simulation, following the Von Mises yielding criterion, as shown in Equation (1):

$$f(\sigma_{ij}) = J_2 - k_2^2 = 0 \quad (1)$$

where k_2 is material constant, and J_2 is Bias stress second invariant:

$$J_2 = \frac{1}{6} [(\sigma_1 - \sigma_2)^2 + (\sigma_2 - \sigma_3)^2 + (\sigma_3 - \sigma_1)^2] \quad (2)$$

The AZ31B magnesium alloy sheet uses the power specified rate equation to describe the rheological behavior, as shown in Equation (3):

$$\dot{\epsilon} = A [\sinh(\alpha \bar{\sigma})]^n \exp[-\Delta H / (RT)] \quad (3)$$

where A is empirical constants, n is stress index, ΔH is transformation activation, R is gas constant, and T is deformation temperature. In this simulation, the equation established by the group for the material was used as shown in Equation (4):

$$\dot{\epsilon} = 1.27 \times 10^{18} [\sinh(0.0219\bar{\sigma})]^{8.94} \exp[-253364 / (8.314T)] \quad (4)$$

The critical damage value is a physical quantity that reflects the tendency of a material to fracture. According to the corresponding fracture criterion, a material cracks when the damage value reaches the critical value of the material. In this paper, the Normalized Cockcroft and Latham fracture criterion was selected, as shown in Equation (5):

$$C = \int_0^{\bar{\epsilon}_f} \frac{\sigma^*}{\bar{\sigma}} d\bar{\epsilon} \quad (5)$$

where $\bar{\epsilon}_f$ is effective fracture strain, σ^* is maximum principle stress, is increment of equivalent strain, $\bar{\sigma}$ is equivalent stress, and C is the fracture threshold, this value varies with temperature. In addition, in this paper, the damage values of AZ31B magnesium alloy at 100 °C, 150 °C, and 200 °C were simulated with reference to the literature [16].

3.3.3. Results Analysis

For the two factors of shear edge clearance and shear temperature, finite element simulations were performed using nine sets of test scenarios designed with the $L_9(3^2)$ orthogonal test table, and the results are shown in Figure 8. The data were processed and compared with the experimental results to obtain the average burnish band height (mm) and burnish band area (mm^2) of the test indexes under nine groups of combined schemes, and the results are shown in Table 6.

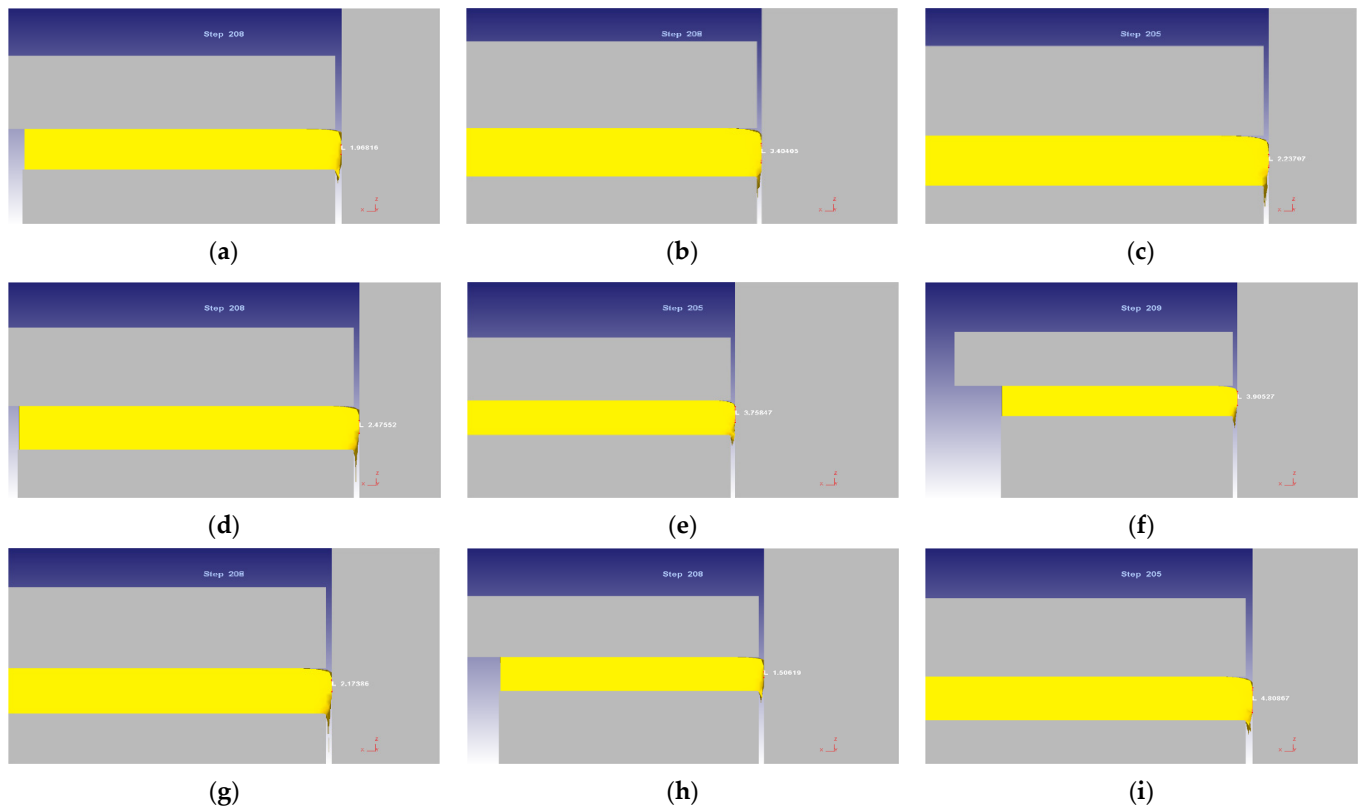


Figure 8. Simulation results: (a) 1-1; (b) 1-2; (c) 1-3; (d) 2-1; (e) 2-2; (f) 2-3; (g) 3-1; (h) 3-2; (i) 3-3. (X–Y refers to factor1–factor2).

From Table 6, it can be observed that, in both the simulation results and experimental results, the R-value of shear temperature is greater than the shear edge gap, that is, the effect of shear temperature on the height of the test index burnish band is greater than the shear edge gap. Therefore, in the shearing process of the magnesium alloy plate, priority is given to the selection of shearing temperature. From the results of this experiment, it can be obtained that 150 °C shear temperature and 12% shear edge clearance can be used as the best processing window for a shearing magnesium alloy plate.

Table 6. $L_9(3^2)$ orthogonal test scheme and simulation results with experimental results.

Test Number	Column Number	1 Blade Clearance	2 Thermal	Simulation Results (mm)	Experimental Results (mm)
1	1	1	1	1.96816	4
2	1	1	2	3.40405	3.9
3	1	1	3	2.23707	1.9
4	2	2	1	2.47552	7
5	2	2	3	3.75847	3.9
6	2	2	2	3.90527	8
7	3	3	3	2.17386	1.1
8	3	3	1	1.50619	5
9	3	3	2	4.80867	8.1

Table 6. Cont.

ColumnNumber HorizontalResult and Range	1	2	1	2
	Blade Clearance	Thermal	Blade Clearance	Thermal
	Simulation Results (mm)	Simulation Results (mm)	Experimental Result (mm)	Experimental Result (mm)
K1	7.60928	5.94987	9.8	16
K2	10.13926	12.11799	18.9	20
K3	8.48872	8.1694	14.2	6.9
k1	2.53643	1.98329	3.27	5.33
k2	3.37975	4.03933	6.3	6.67
k3	2.82957	2.72313	4.73	2.3
R	0.84332	2.05604	3.03	4.37

4. Conclusions

1. In the experiment of warm shear of a rolled AZ31B magnesium plate, the shear edge gap remains unchanged, the height and area of burnish band increases first and then decreases with the rise of shear temperature, and the section quality gradually decreases when the temperature rises to 150 °C. Shear temperature remains unchanged, the height and area of the burnish band increases with the growth of the shear edge gap and then decreases, and the section quality gradually decreases after the shear edge gap reaches 10%. The analysis of the experimental results shows that the best fracture quality is obtained at 150 °C shear temperature with 12% shear gap; the better fracture quality is obtained at the remaining shear temperature with 10% shear gap;
2. Using DEFORM-3D finite element software to simulate the shearing process of magnesium alloy plate and using an orthogonal test method to analyze the results, the study obtained that the influence of the shearing temperature on the height of the burnish band is significantly greater than the shearing edge gap when the rolled AZ31B magnesium plate is sheared in temperature;
3. In this study, the shearing process of a rolled AZ31B magnesium alloy plate gives priority to the selection of shearing temperature, so the shearing temperature of 150 °C and the shear edge clearance of 12% are selected as the best shearing processing window.

Author Contributions: Conceptualization, L.M.; methodology, W.J. and Y.M.; software, Y.M.; validation, W.J. and Y.M.; investigation, Y.M.; writing—review and editing, Y.M. All authors have read and agreed to the published version of the manuscript.

Funding: This work was supported by the National Natural Science Foundation of China (U1910213 and 52105388), the Fundamental Research Program of Shanxi Province (No. 201901D211290), the Key Research and Development Program of Shanxi Province (No. 202102050201005), and the Taiyuan University of Science and Technology Scientific Research Initial Funding (20192002).

Data Availability Statement: The author confirms that the data supporting the findings in this study are available within the article.

Conflicts of Interest: The authors declare no conflict of interest.

References

1. Kahn, R.W.; Shi, C.S.; Ke, J. *Materials Science and Technology Series*; Science Press: Beijing, China, 1999; Volume 8.
2. Ramalingam, V.V.; Ramasamy, P.; Kovukkal, M.D.; Myilsamy, G. Research and development in magnesium alloys for industrial and biomedical applications: A review. *Met. Mater. Int.* **2020**, *26*, 409–430. [[CrossRef](#)]
3. Hao, B.H.; Xia, X.H. Principle of blank shearing and method for improving precision of blank. *Forg. Stamp. Technol.* **2000**, *25*, 3.
4. Rakshith, M.; Seenuvasaperumal, P. Review on the effect of different processing techniques on the microstructure and mechanical behaviour of AZ31 Magnesium alloy. *J. Magnes. Alloy.* **2021**, *9*, 1692–1714.
5. Zhong, Y.B. *Stamping Process and Die Design*; Machinery Industry Press: Beijing, China, 2000.
6. Sagapuram, D.; Efe, M.; Moscoso, W.; Chandrasekar, S.; Trumble, K.P. Controlling texture in magnesium alloy sheet by shear-based deformation processing. *Acta Mater.* **2013**, *61*, 6843–6856. [[CrossRef](#)]
7. Han, T.; Zou, J.; Huang, G.; Ma, L.; Che, C.; Jia, W.; Wang, L.; Pan, F. Improved strength and ductility of AZ31B Mg alloy sheets processed by accumulated extrusion bonding with artificial cooling. *J. Magnes. Alloy.* **2021**, *9*, 1715–1724. [[CrossRef](#)]

8. Fatemi-Varzaneh, S.M.; Zarei-Hanzaki, A.; Beladi, H. Dynamic recrystallization in AZ31 magnesium alloy. *Mater. Sci. Eng. A* **2007**, *456*, 52–57. [[CrossRef](#)]
9. Jang, H.S.; Lee, J.K.; Tapia AJ, S.F.; Kim, N.J.; Lee, B.J. Activation of non-basal $\langle c+a \rangle$ slip in multicomponent Mg alloys. *J. Magnes. Alloy*. **2022**, *10*, 585–597. [[CrossRef](#)]
10. Fan, Y.G.; Wang, L.Y. Medium temperature rheological instability characteristics of AZ31 magnesium alloy. *Chin. J. Nonferrous Met.* **2005**, *15*, 5.
11. Ponge, D.; Gottstein, G. Necklace formation during dynamic recrystallization: Mechanisms and impact on flow behavior. *Acta Mater.* **1998**, *46*, 69–80. [[CrossRef](#)]
12. Yan, Q.S.; Lai, Z.M.; Lu, J.B. Influence of Clearance on Disc Slitting Surface Morphology for Galvanized Steel Sheet. *J. Plast. Eng.* **2014**, *4*, 69–73.
13. Chen, M.H.; Hu, D.C. Research Progresses of Ductile Fracture and Blanked Surface Quality in High speed Blanking. *China Mech. Eng.* **2016**, *27*, 1263–1271.
14. Yin, D.L.; Zhang, K.F.; Wang, G.F.; Han, W.B. Warm deformation behavior of hot rolled AZ31Mg alloy. *Mater. Sci. Eng. A* **2005**, *392*, 320–325. [[CrossRef](#)]
15. Montheillet, F.; Lurdos, O.; Damamme, G. A grain scale approach for modeling steady-state discontinuous dynamic recrystallization. *Acta Mater.* **2009**, *57*, 1602–1612. [[CrossRef](#)]
16. Dong, J.R.; Zhang, D.F.; Dong, Y.F.; Pan, F.S.; Chai, S.S. Critical damage value of AZ31B magnesium alloy with different temperatures and strain rates. *Rare Met.* **2021**, *40*, 137–142. [[CrossRef](#)]